Z. Phys. D – Atoms, Molecules and Clusters 17, 291–298 (1990)

Atoms, Molecules and Clusters
Zeitschrift für Physik D

Chlorine K shell photoabsorption spectra of gas phase HCl and Cl_2 molecules

S. Bodeur *, J.L. Maréchal, C. Reynaud, D. Bazin, and I. Nenner

Laboratoire pour l'Utilisation du Rayonnement Electromagnétique, CNRS, CEA et MEN, Université de Paris-Sud, F-91405 Orsay Cedex, France and
Département de Physique Générale – SPER, Centre d'Etudes Nucléaires de Saclay, F-91191 Gif sur Yvette Cedex, France

Received 12 July 1990

Abstract. High resolution photoabsorption spectra of HCl and Cl_2 have been measured near the chlorine K edge in the 2810–2850 eV photon energy range. Below the Cl K edge, the strongest resonance is interpreted as a simple core excitation into the unoccupied σ^* valence orbital for both molecules, leading to a markedly repulsive state. Higher resonances due to low lying Rydberg states, are observed in both systems, but with a larger oscillator strength for HCl as compared to Cl_2. In Cl_2, the σ^* orbital is deep enough to avoid any mixing with Rydberg orbitals. In HCl, we observe the dipole forbidden Cl $1s \rightarrow 4s$ transition which denotes a strong $4s-4p$ hybridization. Above the Cl K edge, the multiplet features seen for HCl are analysed in terms of double-core-valence excited vacancy states. In Cl_2, their counterpart are found very close to the ionization threshold because of the deep σ^* orbital and possibly because the excited core and valence electrons originates either from the same atomic site or from different ones.

PACS: 33.20.Rm

I. Introduction

K-shell Photoabsorption Spectroscopy or Electron Energy Loss Spectroscopy of gas phase molecules bring the opportunity to probe core electronic states without interference with other core or valence excitation channels. The general resonance pattern, at least those corresponding to one electron transitions both in the discrete and the continuum spectra, can be understood using molecular terms rather than atomic ones because *i)* the lowest unoccupied orbitals antibonding valence σ^* or π^* reflect the bonding of the absorbing atom with its neighbours *ii)* the low lying Rydberg orbitals have quantum defects which do not fit typical atomic values or their relative high oscillator strength is often due to their mixed valence character *iii)* the anisotropy of the molecular potential affects the ionization of the K-shell electron and is responsible for the observation of shape resonances.

Of particular interest are hydrides built with second row elements like HCl, H_2S, PH_3 and SiH_4 which shows very rich $2p$ photoabsorption spectra [1–5] in contrast with the argon spectrum [6, 7]. In this isoelectronic series, there is a continuous change from valence to Rydberg type of orbitals [8, 9]. The lowest valence orbital, σ^*, incorporates some s-Rydberg character as it rises in energy from HCl to SiH_4. In SiH_4, the strong valence-Rydberg mixing explains the rather high intensity of low lying Rydberg states in both the Si $2p$ [7, 8] and Si $1s$ [10] spectra. This valence-Rydberg mixing disappears in $SiCl_4$ [10] and consequently, the true Rydberg states have no oscillator strength. On the other hand, in going from HCl to SiH_4, the molecular potential becomes more symmetrical, so that the $s-p$ mixing of the Rydberg orbital decreases to zero. This explains the high intensity of the dipole forbidden transition to the $4p$ orbital observed in the $2p$ photoabsorption spectrum of HCl [1, 3–5].

The Cl $2p$ photoabsorption spectrum of the Cl_2 molecule [3, 5, 11] shows marked differences as compared to the Cl $2p$ spectrum of HCl. The comparison of K-shell spectra of HCl and Cl_2 molecules offers the opportunity to analyse the σ^* and Rydberg orbitals through the term values and oscillator strengths of the corresponding core excited states, when a chlorine atom is found in two different bonding situations. Calculations of term values [3, 9, 12] and oscillator strength [3] have been made of σ^* and Rydberg states in the K-shell spectrum of HCl. Similarly, calculations on the Cl $2s$ [3] and Cl $2p$ [13] spectra of Cl_2 are also available. A strong σ^* state is predicted with two low lying $4s\sigma$ and $4p\pi$ Rydberg states but with quite different oscillator strength in going from HCl to Cl_2.

In the present paper, we report photoabsorption measurements in HCl and Cl_2, in the region around

* On leave from Laboratoire de Chimie Physique, 11 rue Pierre et Marie Curie, 75231 Paris Cedex 05, France

the chlorine K edge, in a more extended range (2810–2850 eV) and using higher resolution than previous measurements [14–17]. We report the observation of valence and several new Rydberg states with large differences between the two molecules. We offer an interpretation of the discrete resonances on the basis of previous calculations [3, 9, 12, 13] and comparison with the Cl $2p$ experimental spectrum [1, 3–5, 11]. We discuss the correlation between the bond character, the bond strength and the energy of the σ^* orbital, as well as the importance of the valence-Rydberg mixing and the $s-p$ hybridization of Rydberg orbitals. We also report new fine structures in the continuum for both molecules. We interpret them in terms of doubly excited states, in which, in addition to the K shell excitation, a valence electron of the chlorine atom is excited. We discuss, in the specific case of Cl_2, the presence of localized or delocalized doubly excited states, respectively on a single chlorine site or on both.

II. Experimental

Photoabsorption spectra have been obtained at LURE, the French synchrotron radiation facility, on the EXAFS IV station implanted on the DCI storage ring. DCI is operated with positrons of 1.85 GeV with an average current of 300 mA. The experimental set-up is schematically represented in Fig. 1. X-ray absorption spectra have been recorded using a double crystal monochromator equipped with two silicon (111) crystals ($2d = 6.271$ Å). In addition, we have used a set of two reflecting mirrors for high harmonics rejection [18].

The monochromatic beam passes through a 205 mm long cell filled with the gas under consideration, which is limited by two 13 mm diameter windows made of 12 μm thick propylene polyfilm. The transmission of polypropylene is better than 80% in our spectral range [19]. The detection of the incident and transmitted beam is ensured simultaneously, using two ionization chambers. The gas inlet system is built with stainless steel and metallic gaskets in order to minimize damage from corrosive gases. In order to eliminate residual water vapor, we have baked out the cell and inlet system, then we have flushed it repeatedly with $Si(CH_3)_3Cl$ vapor before pumping it again.

Spectra were obtained by scanning the photon energy automatically, in choosing small steps of 0.1 to 0.2 eV for measuring reliably all possible fine structures within the limit of the resolving power. Typical recording times for a full spectrum were of the order of 30 min.

The photon wavelength scale is given by the measurement of Bragg angles and accurate calibration by recording the $CHCl_3$ gas spectrum, near the Cl $1s$ edge. The most intense valence transition located at 2823.5 eV [20] is taken as the energy reference. We estimate then that the accuracy of the absolute energy scale amounts to 0.5 eV and the accuracy for the relative energies of sharp features within a single spectrum to be better than 0.1 eV.

HCl and Cl_2 gases are commercially available from Prodair Company with a purity of 99.8%. They are introduced in the cell without further purification other than a passivation of the system by repeated flushing cycles with the gas under study. Spectra are recorded with a pressure of 5 torrs stabilized within 1%, as measured with a capacitance manometer. This pressure was chosen to be low enough to avoid absorption saturation [21] and high enough to obtain the best contrast between the spectral features and the continuum.

In order to obtain absolute cross sections (σ), we have used the following procedure. Firstly, we have selected several photon energies, for which we have measured the transmitted intensity through the full (I) and empty (I_0) cell, with a single detector. We have then eliminated the absorption of the polypropylene windows. Secondly, knowing the density ρ_0 of the gas under normal conditions of pressure and temperature (P_0 and T_0) i.e. $\rho_0 = 1.00045$ g/l for HCl and 3.214 g/l for Cl_2, we have extracted the absolute photoionization cross section, per molecule, from the following formula:

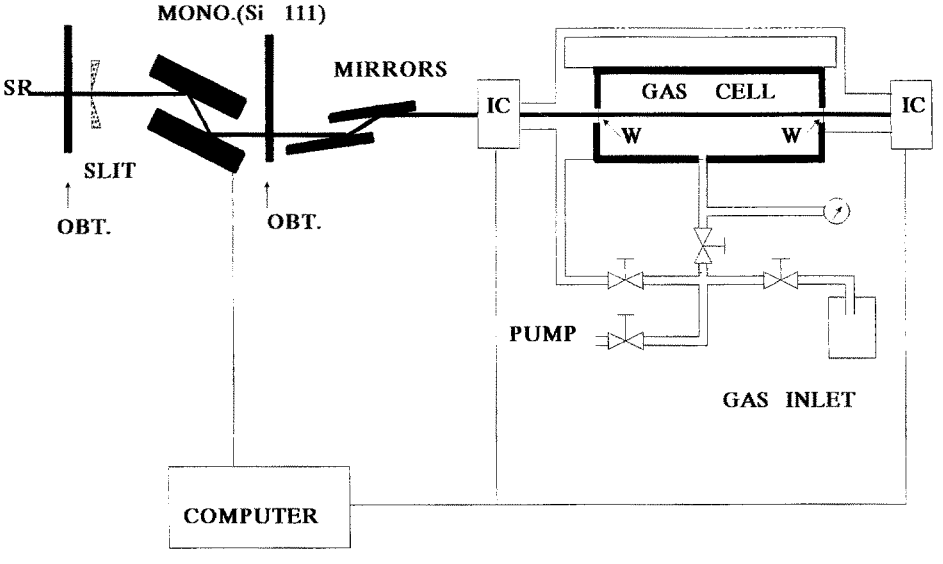

Fig. 1. Schematics of the experimental set-up; SR: synchrotron radiation; Obt: obturator; Mono: monochromator; IC: ionization chamber; W: (Polypropylene) windows

$$\sigma(\text{Mb}) = \frac{M}{N}\frac{1}{\rho_0 x}\frac{P_0}{P}\frac{T}{T_0}\,\text{Ln}\frac{I_0}{I}$$

with N being the Avogadro number, M the molecular weight, P and T the pressure and temperature in the present experimental conditions and x the cell length.

III. Results and discussion

We show in Figs. 2 and 3, photoabsorption spectra of HCl and Cl_2 near the chlorine edge. The enlargement on each figure is made to see details of the weak features observed superimposed in the continuum. In the case of Cl_2, we paid a specific attention to the resonances in the discrete region, because unlike of the previous results [14–17], we do not observe a resonance some 2 eV above the main one. We believe that this spurious structure reported in [14–17] is due to an impurity probably a chlorohydrocarbon. Indeed, at this specific photon energy, we could also detect this additional peak only if the cell and inlet system were not properly conditioned. Furthermore, we have analysed the pressure dependence of its relative intensity and we confirm that the extra peak of [14–17] does not belong to the Cl_2 spectrum. This conclusion is in agreement with the results reported at the $2p$ edge [3, 11]. We have indicated in both figures the energy of the chlorine K edge, as extracted from the addition of the K_α emission line of the chlorine atom [22] plus the chlorine $2p$ binding energy obtained from high resolution Electron Energy Loss Spectroscopy [4, 11] rather than X-ray Photoelectron Spectroscopy [23] because of higher accuracy. The energies, widths, term values and peak intensities have been reported in Tables 1 and 2, respectively for HCl and Cl_2.

From the analysis of Figs. 2 and 3, we observe that the order of magnitude of the cross section lies in the range of 0.1 to 0.8 Mb, and this is around 20 times smaller than the cross section in the Cl $2p$ region [3]. This ratio fits the calculated one extracted from atomic cross sections for the third row elements when one chooses 20 eV excess energy above each ionization onset [24]. More interestingly, we observe that, out of the resonance region, that is some 20 eV above the ionization edge, the cross section for Cl_2 is the double than those

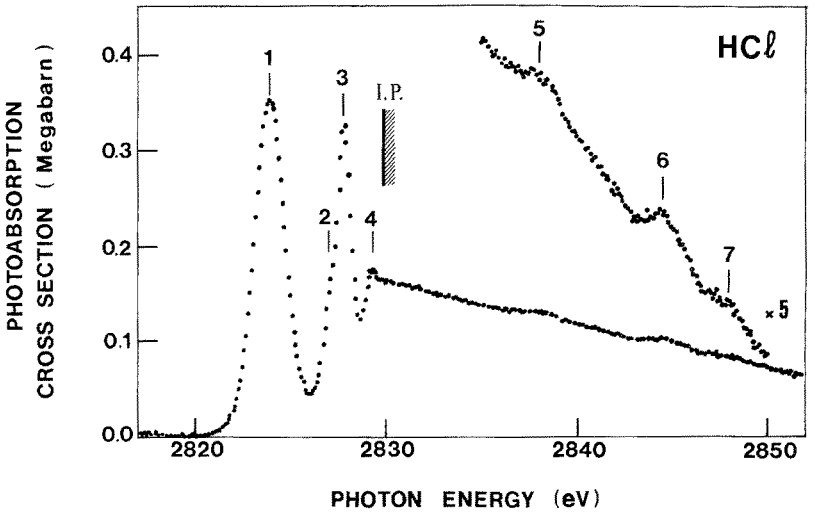

Fig. 2. Photoabsorption spectrum of HCl in the 2810–2850 eV range with details of the double core-valence vacancy states. For assignments, see Table 1

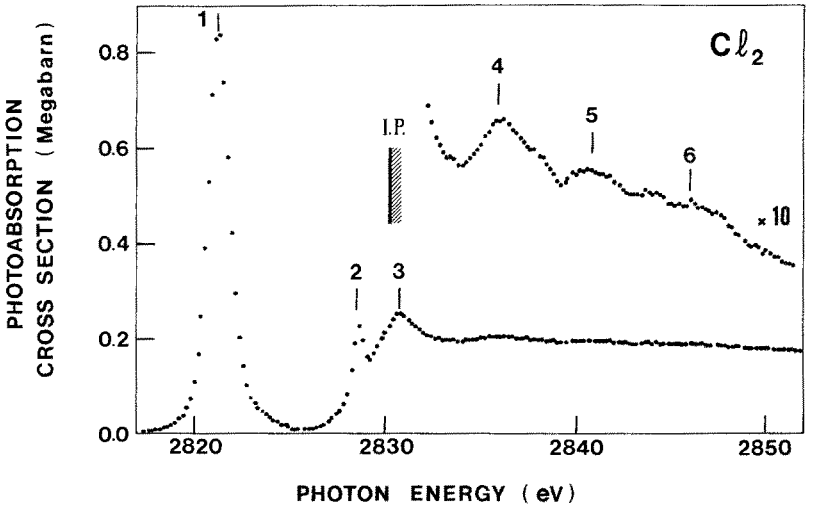

Fig. 3. Photoabsorption spectrum of Cl_2 in the 2810–2850 eV range with details of the double core valence vacancy states. For assignments, see Table 2

Table 1. Energies, term values, energies relative to the σ^* transition, widths, intensities and suggested assignment of K-edge resonances in HCl

Peak	Energy (eV)	Term value (eV)	Energy relative to the σ^* (eV)	Width (FWHM) (eV)	Intensity (Mbarn. eV)	Assignment
1	2823.9	+5.9	0	1.86	0.75	$3p\sigma^*$
2	2827.0	+2.8	3.1	0.84	0.11	$4s\sigma$
3	2827.8	+2.0	3.9	0.84	0.29	$4p\pi$, $4p\sigma$
4	2829.3	+0.5	5.4			$5p\pi$, $5p\sigma$
IP[a]	2829.8	0				
5	2838	−8.2	14.1			doubly
6	2844.5	−14.7	20.6			excited
7	2848	−18.2	24.1			states

* The ionization potential (IP) is the sum of the Cl $2p$ binding energy from [4], and the chlorine K_α emission line, from [22]

Table 2. Energies, term values, energies relative to the σ^* transition, widths, intensities and suggested assignment of K-edge resonances in Cl_2

Peak	Energy (eV)	Term value (eV)	Energy relative to the σ^* (eV)	Width (FWHM) (eV)	Intensity (Mbarn. eV)	Assignment
1	2821.3	+8.9	0	1.36	1.44	$3p\sigma_u^*$
2	2828.5	+1.7	7.2	0.7	0.13	$4p/3d$
IP[a]	2830.2	0				
3	2830.8	−0.6	9.5			doubly
4	2836	−5.8	14.7			excited
5	2841	−10.8	19.7			states
6	2846	−15.8	24.7			

* The ionization potential (IP) is the sum of the Cl $2p$ binding energy from [11], and the chlorine K_α emission line, from [22]

of HCl. This is readily interpreted as being due to the number of chlorine atoms. In the resonance region, the comparison between absolute cross sections of both molecules is meaningless because the nature of the transitions depends upon the unoccupied valence and Rydberg orbitals, which are obviously different for each system.

The electronic configuration of ground state HCl is

$$\underbrace{1s\sigma^2\ 2s\sigma^2\ 2p\sigma^2\ 2p\pi^4}_{\text{Cl core orbitals}}\quad\underbrace{3s\sigma^2\ 3p\sigma^2\ 3p\pi^4\ 3p\sigma^{*0}}_{\text{valence orbitals}}$$

The electronic configuration of ground state Cl_2 is

$$\underbrace{1s\sigma_g^2\ 1s\sigma_u^2\ 2s\sigma_g^2\ 2s\sigma_u^2\ 2p\sigma_g^2\ 2p\sigma_u^2\ 2p\pi_g^4\ 2p\pi_u^4}_{Cl_2\text{ core orbitals}}$$

$$\underbrace{3s\sigma_g^2\ 3s\sigma_u^2\ 3p\sigma_g^2\ 3p\pi_u^4\ 3p\pi_g^4\ 3p\sigma_u^{*0}}_{\text{valence orbitals}}$$

We now analyse the various structures in both spectra in considering separately the discrete region and the ionization continuum.

A. Valence and Rydberg states

The lowest resonance seen in the spectra of Figs. 2 and 3 are the strongest and also the widest (FWHM = 1.9 eV for HCl and 1.4 eV for Cl_2). They are readily interpreted in terms of a $1s \rightarrow 3p\sigma^*$ state, because the lowest unoccupied orbital is valence antibonding for both HCl and Cl_2. We find that the σ^* term value is 3 eV higher in Cl_2 than in HCl (see Tables 1 and 2). They are followed by one or several sharper peaks due to transition to Rydberg molecular orbitals. They are by far, much richer and more intense in HCl than in Cl_2. These observations have been made also for the Cl $2p$ edge spectra [1, 3–5, 11], as seen in Tables 3 and 4. Interestingly, these differences are also apparent when one compares the HF and F_2 spectra [25] measured near the F $1s$ edge, as well as the HBr and Br_2 ones [4] recorded near the Br $3d$ edge. Because it is a common character to HX and X_2 molecules for three halogen X atoms, we believe that this is due to the very different nature of the bond between the homonuclear X_2 and heteronuclear HX molecules. The bond strength is much higher in HX (5.94, 4.43 and 3.8 eV for X = F, Cl and Br respectively [26]) than in X_2 (1.6, 2.48 and 1.97 eV for X = F, Cl and Br respectively [26]). The greater difference in the σ^* term value is observed for X = F (6.7 and 14.5 eV for HF and F_2 respectively [25]) and corresponds to the greater difference in the bond strength. Such a relation between bond strength and σ^* position is due to the fact that both quantities depend on the overlap between the atomic orbitals involved in the bonding. This overlap is greater in HX than in X_2.

Table 3. Term values (eV) and assignment of the $2p3/2$ edge resonances in HCl observed or calculated by different authors

	Experimental results			Theoretical results	
	Ref. 3	Ref. 4	Ref. 1	Ref. 9	Ref. 3
σ^*	5.8	6.4	6.2	5.8	5.35
$4s$	2.91	3.4	3.15	2.85	2.84
$4p$	2.13	2.7	2.35	2.52–2.32	2.37
$3d$		1.86	1.7	1.53–1.46	1.53
$5s$	1.27	1.64	1.5	1.29	
$5p$		1.26	1.2	1.19–1.13	
$4d+6s$		0.98	0.8		
IP (eV)	207.3	207.3	207.4		

Table 4. Term values (eV) and assignment of the $2p3/2$ edge resonances in Cl_2 observed or calculated by different authors

	Experimental results			Theoretical results	
	Ref. 3	Ref. 11	Ref. 5	Ref. 13	Ref. 3
σ^*	9.4	9.5	9.7	9.47	8.1
$4s$	3.5	3.56	3.8	3.14	3.14
$4p$	2.28	2.4	2.35	2.2	2.14
$3d$	1.7	1.8	1.9	1.5	1.31
$5s$	1.46		1.57	1.4	1.55
IP (eV)	208.3	207.8	208.0		

The σ^* orbital position influences the valence-Rydberg mixing. In Cl_2, the σ^* is deep enough to avoid any mixing with Rydberg orbitals. In HCl, this is not the case and, although the Rydberg-valence mixing is weaker in HCl compared to the other hydrides [8, 9], as discussed in the introduction, some mixing may nicely explain that Rydberg states are observed with a larger oscillator strength in HCl compared to Cl_2.

The cross section measured at the σ^* resonance as compared to the continuum is very large for both molecules (Figs. 2 and 3) in contrast to the observations in the Cl $2p$ spectra [1, 3–5, 11]. We explain these observations by the fact that the σ^* orbital is mainly built with $3p$ atomic orbital. Consequently, one expects large matrix elements for K shell excitation because of electric dipole selection rules.

The width of the σ^* resonance (Tables 1 and 2) is larger for each molecule (by an amount of 0.5 to 0.6 eV) than observed at the $2p$ edge [1, 3–5, 11]. This is due to *i)* the better resolution achieved in the 180 eV energy region by both photoabsorption (0.07 eV at 200 eV) or Electron Energy loss technique (0.075 eV quoted in [4] and 0.065 eV in [11]), as compared to photoabsorption in the 2800 eV range (0.4 eV in the present work) *ii)* the higher natural width of the $1s$ hole (0.4 eV as reported in [27]) compared to the $2p$ (0.1 eV as reported in [27]). In addition, for each molecule, the width of the σ^* resonance is found much larger than the width of Rydberg transitions, regardless the nature of the inner hole. This is due to the strongly antibonding character of the final orbital which opposes itself to Rydberg orbitals which are mainly non bonding. In other words, the width is essentially due to the repulsive character of the core excited state leading to a large Franck-Condon envelope of the core excited state rather than lifetime effect. Because both the resolution and lifetime broadening are contributing to the observed width, we could not attempt to make a reliable deconvolution and give an accurate number for the Franck-Condon envelope. We can only conclude that our present results are fully compatible with the results of Shaw et al. [4, 11] near the $2p$ edge of chlorine. Another way to look at the origin of the large width of σ^* resonances is to describe this core excited state as its core equivalent species, as done before by Shaw et al. [4, 11] and by Schwarz [9]. For HCl the core equivalent molecule is ArH and for Cl_2, it is ArCl. The ground state of these excimers is essentially a repulsive potential curve. An important prediction about the decay of such resonances should be made at this point. In HCl, the fragmentation of σ^* into H + Cl* is likely to compete efficiently with the electronic $1s$ hole relaxation i.e. the Auger decay. Such unexpected fast fragmentation processes already established for HBr [28] or HI [29] should also exist for HCl. In contrast, in Cl_2, the fragmentation of σ^* into Cl + Cl* should not play a significant role because of the unfavorable mass ratio of the fragments [28].

The Rydberg transitions correspond to the peaks labelled 2, 3 and 4 in HCl and 2 in Cl_2. The enlarged spectrum of Fig. 4 (HCl) shows clearly that the peaks 2 and 3 are partially resolved. Figure 4 shows also the deconvoluted peaks from which we could extract the partial widths and relative intensities reported in Table 1. Notice that this deconvolution is satisfactory only if we account for a small, but unresolved structure between peak 1 and 2. We believe that it originates in an assym-

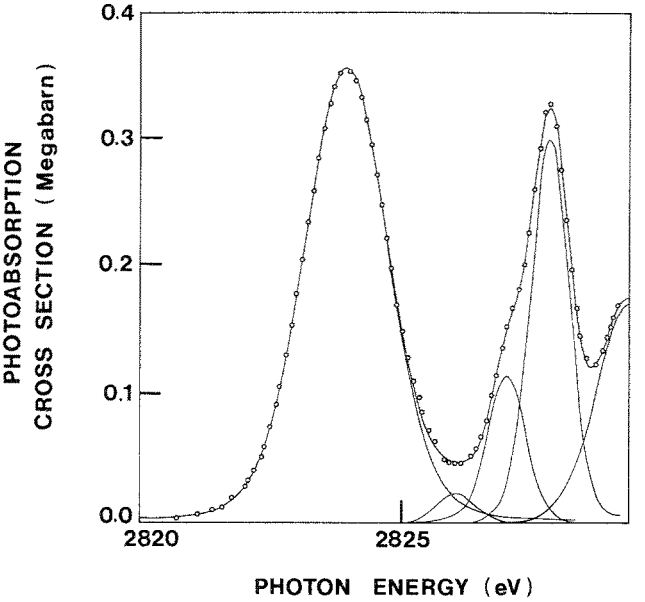

Fig. 4. Detail of the photoabsorption spectrum of HCl in the 2820–2830 eV range. Circles are the experimental points. Full lines represent the results of a least-square deconvolution procedure using linear combination of a gaussian and a lorentzian functions as line shape. Intensities and widths deduced from this procedure are reported in Table 1

metric shape of peak 1, which has not been taken into account in the deconvolution procedure. Considering only the resolved peaks, they are clearly narrower than the σ^* resonance and rather intense, although significantly smaller than the main resonance. In Cl_2, the width of peak 2 amounts of 0.7 eV i.e. a value somewhat smaller than the width of HCl Rydberg states (0.84 eV). This favors again an interpretation in terms of some admixture of a valence character in the Rydberg orbitals of HCl, which should induce a distorted potential energy curve. It is difficult to extract the Franck-Condon width, especially in the absence of XPS data of the chlorine $1s$ line. Calculations would be welcome to clarify this point.

The question is to assign precisely the Rydberg states of Figs. 2 and 3. For this purpose we are comparing (see Tables 3 and 4) the term values and relative intensity of peaks as measured in the present work with the $2p$ experimental spectra [3–5, 11]. We also use the calculations of Schwarz [9], Kondratenko et al. [13] and Ninomiya et al. [3]. However, the ordering of $np\pi$, $np\sigma$, $ns\sigma$, $nd\pi$, $nd\sigma$ is not always well established because the energy separation between states is smaller than the accuracy of the calculations. Oscillator strengths are more useful for a more precise assignement but such calculations are only offered in [3].

In the HCl spectrum, peak 3 is the most intense Rydberg resonance and we favor a $4p$ assignment because of favorable matrix element from K shell excitation. In addition, the energy separation between peak 3 and σ^* is equal to 3.9 eV, in agreement with the values obtained at the Cl $2p$ edge 3.7 eV [3] and 3.7 eV [4], as seen in Table 3. The case of peak 2 is rather clear. It is separated from the σ^* peak by 3 eV in agreement with [3] (2.9 eV) and [4] (3 eV), if we assign it as due to the $1s \rightarrow 4s\sigma$ transition. Notice that if we make the same comparison with term values, i.e. taking the ionization potential as a reference, we obtain a better agreement with the experimental results of [3] (shift of 0.1 eV). When comparing with the results of [4], our term values are smaller by 0.6 eV. Since the Cl $1s \rightarrow 4s$ transition is forbidden by the electric dipole selection rules, the intensity of the $4s\sigma$ peak is probably due to its p character [8]. In the $2p$ photoabsorption spectra, such $4s-4p$ hybridization explains the intensity of the forbidden $2p \rightarrow 4p$ transition [1, 3–5]. However, Ninomyia et al. [3] have calculated at the $1s$ level, a larger intensity for the $4s$ as compared to the $4p$ state and this is surprising, unless the strong hybridization of the orbitals is such that atomic type of reasoning is not correct. Finally, the interpretation of peak 4 is not possible since the accuracy of term values and oscillator strengths predicted by theory [3, 8] is not sufficient considering the number of possible candidates ($5p$ or $3d$) and the discrepancies between the different experimental results [1, 3, 4].

For Cl_2, we observe a single Rydberg peak. We have offer that it is due to $1s \rightarrow 4p$ transition. This is based on the experimental Cl $2p$ spectra reported by Ninomyia et al. [3] and by Shaw et al. [11], in which the $4p$ Rydberg state is located 7.1 eV above the σ^* state, see Table 4. This energy difference equals 7.2 eV in the Cl $1s$ spectrum and this supports our interpretation. However, our present term value is smaller by 0.5 to 0.6 eV with respect to the values of [3] and [11]. This makes this interpretation ambiguous since both $4p$ and $3d$ could be invoked. The theoretical calculations of [3, 13] give very close numbers for term values which fit the experimental $2p$ results [3, 11]. But the accuracy of this calculations is not sufficient to discuss further the term values. The calculations of relative intensities of Ninomyia et al. [3] predict a dominant contribution of the $4p$ state and a small (but not negligible) for the $3d$ state. This favors again an interpretation in term of a $4p$ state. The shape of the spectrum (Fig. 3) around the ionization edge is quite different from those of HCl (Figs. 2 and 4). It seems that there is an unresolved background which is superimposed on the direct ionization step. We cannot rule out a contribution of other small and wide Rydberg states which could not be resolved because of the $1s$ lifetime effect and experimental resolution. It is also possible that we deal with a single broad resonance extending below the ionization potential. The interpretation of this feature is discussed in the next section.

B. Double-core-valence vacancy excited states

The HCl and Cl_2 spectra of Figs. 2 and 3 show weak and relatively narrow structures in the $1s$ ionization continuum, which are reported for the first time. In HCl, they are labelled 5, 6 and 7 and their energies are reported in Table 1. In Cl_2, they are labelled 4, 5 and 6, although each identified structure is certainly made of many unresolved components. Their energies are reported in Table 2. We interpret them as due to multiple electron effects because of the following.

In hydrides, we do not expect intense shape resonances because the departing electron is only weakly backscattered by the neighbouring hydrogen atoms. Consequently, the K-shell ionization continuum of the heavy atom has a general monotonous decreasing behavior and any structure (especially narrow one) is essentially due to multi-electron effects. This is the case of the sulfur K-edge spectrum of H_2S [30] or the silicon K-shell photoabsorption spectrum of SiH_4 [10]. In HCl which is isoelectronic of these molecules, the observations are similar. In the absence of any detailed calculation on the energy or intensity of double-core vacancy states, we take the argon atom as a starting point of our interpretation.

In argon, numerous double core-valence excitation features have been observed 40 eV above the $1s$ ionization edge. A first group of structures appears as the most intense ones and has been interpreted [31] as due to the simultaneous excitation of the core and $3p$ electron. The second group observed with much weaker intensity, some 12 eV above the first group, is due also to double core-valence excitation but involving a $3s$ inner valence electron. Very detailed interpretation of the most intense resonances (first group) has been revisited by Cooper [32]. The main resonance is due to the $1s\,3p^5\,3d^2$ configuration. The other structures below and above this reso-

nance is due to different states with the $1s\,3p^5\,4p^2$ configuration either reached directly or via mixing with the $3d^2$ configurations. Because in the analysis of Cooper [32], there is no clear cut between initial and final state correlation effects, we are assuming in the following that both are present in the molecules under study, without any other hypothesis. Consequently, we discuss the results using energetic arguments only.

In the case of HCl, if the fine structures of Fig. 2 are the counterpart of those of argon, it is striking that they are found at much lower energy and with much higher intensity. Considering that the σ^* orbital is largely deeper than any of the Rydberg orbitals in argon, we expect the $1s\,3p\pi^3\,\sigma^{*2}$ or $1s\,3p\sigma\,\sigma^{*2}$ configurations to give the lowest group of structures. However, the ultra violet photoabsorption spectrum of HCl [32] or the Electron Energy Loss Spectrum [4] shows that there is a structure due to the $3p\pi \rightarrow \sigma^*$ transition, but it is extremely broad compared to Rydberg states. It is then plausible to expect that the doubly excited state with two electrons in the σ^* orbital will also give an even broader peak smeared out in the continuum. The other states due to $1s\,3p\pi^3\,\sigma^*\,4p$, $1s\,3p\sigma\,\sigma^*\,4s$, $1s\,3p\pi^3\,4p^2$, $1s\,3p\sigma\,4p^2$, $1s\,3p\pi^3\,4s\,4p$, $1s\,3p\sigma\,4s\,4p$, $1s\,3p\pi^3\,4s^2$ or $1s\,3p\sigma\,4s^2$ configurations must be considered more favourably.

Let us compare the energy of peaks 5 in HCl with the energy of 4 in Cl_2. Because we deal with double excitation features, the term value is no more relevant for the comparison. We rather take the energy difference with the σ^* resonance and the corresponding numbers are reported in Tables 1 and 2. It is quite interesting to observe that these values are very similar from one molecule to the other. Generally we expect that this relative energy ΔE_i compared to the energy of the main $1s \rightarrow \sigma^*$ resonance to be given by

$$\Delta E_{v \rightarrow v^*} = \varepsilon_{v \rightarrow v^*} + \mathcal{J} + \mathcal{K} + \mathcal{C}$$

where $\varepsilon_{v \rightarrow v^*}$ is the valence excitation energy, $\mathcal{J}$ is the Coulomb term, $\mathcal{K}$ the exchange term and $\mathcal{C}$ the correlation contribution. Firstly, the fact that in both molecules, the mean value of ΔE is much smaller than in the argon case reflects that the $\mathcal{J}$ term is much smaller in molecules than in atoms. This is because in molecules, occupied and unoccupied valence (even low Rydberg) are more delocalized or diffuse and the two holes found in a K shell and in the valence shell are very likely not to be found on the same atom and this immediately makes the Coulomb term much smaller.

We turn now to the comparison between both molecules. The lower ε_{v-v^*} value corresponds to transition from $3p\pi$ orbital in HCl and $3p\pi_g$ in Cl_2 to Rydberg orbital $4s$ or $4p$ and is about 9 eV in both cases ([33] and [4] for HCl and [34] for Cl_2). If we consider in the first place that the $\mathcal{J}$, $\mathcal{K}$ and $\mathcal{C}$ terms are equal, then it is not surprising that the ΔE values are equivalent and the fact that doubly excited states are closer the ionization threshold, than in HCl, is simply due to the deeper σ^* in Cl_2 compared to HCl. The same reasoning is possible for peaks 6 and 7 in HCl compared to peaks 5 and 6 in Cl_2 if we invoke deeper valence states. However, any direct relation with the position of these states can be done because the $\mathcal{J}+\mathcal{K}+\mathcal{C}$ term is expected to be different when the valence hole is changed. Of course, this assignement is only tentative since there must be a contribution of structures due to excitation plus ionization which are difficult to estimate without calculations.

In the above analysis, we have implicitely assumed that the valence orbitals are the same in the fondamental neutral state and in the core excited state. In other words, the valence orbitals are frozen. This means that in Cl_2, the two chlorine atoms are strictly equivalent. However, the presence of the $1s$ hole induces a polarization of valence orbitals, including the $3p$ lone pairs. The description in a broken symmetry model, which is good for a single core excitation (the core equivalent model is valid), is also good for the additional valence excitation. Therefore, we should expect two families of double excited states. One in which the two holes are found on a single chlorine site (type I) and another in which the two holes are found on different sites (type II). The energy difference would essentially be found in the $\mathcal{J}$ Coulomb term which would be smaller for the second situation. This delocalization effect has been predicted by Cederbaum et al. [35] for two core vacancy states in hydrocarbon molecules. Consequently, if this double excited state is of type II, it should appear at lower energy than those of type I. Turning now to the spectrum of Fig. 3, we can consider that the Cl_2 spectrum has a contribution of both types of doubly excited states and peak 3 is a possible candidate for a type II state, whereas, the peaks labelled 4, 5 and 6 which have their counterpart in HCl are of type I. This tentative interpretation needs obviously to be checked by theory, especially because, in this molecule, we cannot avoid the presence of a very low lying shape resonance because unlike in HCl, the ejected $1s$ electron from one chlorine atom experiences the presence of the neighbouring atom.

IV. Conclusions

The chlorine K-shell photoabsorption spectra of HCl and Cl_2 shows that the lowest antibonding orbital σ^* is deeper in the Cl_2 molecule than in HCl. This is fully consistent with the difference in the bond strength of the molecules and is a characteristic of all the halogen atoms. In HCl the low lying Rydberg orbital have a valence character and are strongly hybridized, with large oscillator strengths and rather large widths. In contrast, in Cl_2, the oscillator strength of the Rydberg states is weak.

Doubly excited states are observed in both systems. They are due to the simultaneous excitation of a $1s$ electron and a valence electron. The Coulomb term is surprisingly very small, compared to any atomic situation. They are even found much closer to the ionization threshold in Cl_2 because the σ^* orbital is deeper. We offer to interpret the richer spectrum of Cl_2 in considering the existence of two sets of doubly excited states,

essentially because the core hole induces a strong polarization of the outer valence orbitals, especially lone pairs. The main consequence of this is a symmetry broken description of the states, in which one should consider separately holes located on the same atomic site or on different sites. It is offered that a rather intense resonance located right at threshold is a candidate for such a delocalized double-core-valence vacancy excited state.

We are thanking Philippe Millié and Paul Morin for very helpful discussions and we are grateful to the LURE staff for operating the DCI ring and for general facilities.

References

1. Hayes, W., Brown, F.C., Kunz, A.B.: Phys. Rev. Lett. **27**, 774 (1971); Hayes, W., Brown, F.C.: Phys. Rev. A **6**, 21 (1972)
2. Ishiguro, E., Iwata, S., Mikuni, A., Susuki, Y., Kanamon, H., Sasaki, T.: J. Phys. B **20**, 4725 (1987)
3. Ninomiya, K., Ishiguro, E., Iwata, S., Mikuni, A., Sasaki, T.: J. Phys. B. Atom. Mol. Phys. **14**, 1777 (1981)
4. Shaw, D.A., Cvejanocic, D., King, G.C., Read, F.H.: J. Phys. B **17**, 1173 (1984)
5. Gluskin, E.S., Krasnoperova, A.A., Mazalov, L.N.: Zhur. Strukt. Klimii **18**, 665 (1977)
6. Nakamura, M., Sasanuma, M., Sato, S., Watanabe, M., Yamashita, H., Iguchi, Y., Ejiri, A., Nakai, S., Yamagushi, S., Sagawa, T., Nakai, Y., Oshio, T.: Phys. Rev. Lett. **21**, 1303 (1968)
7. King, G.C., Tronc, M., Read, F.H., Bradford, R.C.: J. Phys. B **10**, 2479 (1977)
8. Schwarz, W.H.E.: Chem. Phys. **9**, 157 (1975)
9. Schwarz, W.H.E.: Chem. Phys. **11**, 217 (1975)
10. Bodeur, S., Millié, P., Nenner, I.: Phys. Rev. A **41**, 252 (1990)
11. Shaw, D.A., King, G.C., Read, F.H.: J. Phys. B **13**, L723 (1980)
12. Sukhorukov, V.L., Yavna, V.A., Demekhin, V.F.: Bull. Acad. Sci. USSR, Phys. Ser. **46**, 131 (1982)
13. Kondratenko, A.V., Mazalov, L.N., Neyman, K.M.: Theor. Chim. Acta (Berl.) **54**, 179 (1980)
14. Lindh, A.E., Nilsson, A.: Ark. Mat. Astron. Fis. **29A**, 27, 1 (1943)
15. Stephenson, S.T., Krogstad, R., Nelson, W.: Phys. Rev. **84**, 806 (1951)
16. Sadovskii, A.P., Bertenev, V.M., Blokhin, S.M.: Theor. Chem. **4**, 342 (1968);
Blokhin, S.M., Sadovskii, A.P., Dolenko, G.N., Bertenev, V.M.: J. Struct. Chem. **10**, 722 (1969)
17. Hanus, M.J., Gilberg, E.: J. Phys. B **9**, 137 (1976)
18. Saintavict, Ph.: Thèse de Doctorat, Université d'Orsay (1988); Saintavict, Ph., Petiau, J., Manceau, A., Rivallant, R., Belakowsky, M., Renaud, G.: Nucl. Instrum. Methods Phys. Res. A **273**, 423 (1988)
19. Bodeur, S.: Thèse de Doctorat, Université Pierre et Marie Curie, Paris (1986)
20. Hitchcock, A.P., Bodeur, S., Tronc, M.: Chem. Phys. **115**, 93 (1987)
21. Parratt, L.G., Hempstead, C.F., Jossen, E.L.: Phys. Rev. **105**, 1228 (1957)
22. Cauchois, Y., Sénémaud, C.: Int. Tab. of Sel. Const. **18**. Oxford: Pergamon Press 1978
23. Perry, W.B., Jolly, W.L.: Inorg. Chem. **13**, 1211 (1974)
24. Yeh, J.J., Lindau, I.: At. Data Nucl. Data Tables **32**, 1–155 (1985)
25. Hitchcock, A.P., Brion, C.E.: J. Phys. B **14**, 4399 (1981)
26. Molecular spectra and molecular structure IV: constants of diatomic molecules. Huber, K.P., Herzberg, G. (eds.) New York: Van Nostrand Reinhold 1979
27. Krause, M.O.: J. Phys. Chem. Ref. Data **8**, 307 (1979)
28. Morin, P., Nenner, I.: Phys. Rev. Lett. **56**, 1913 (1986)
29. Morin, P., Nenner, I.: Phys. Scr. T **17**, 171 (1987)
30. Hormes, J., Kuetgens, U., Ruppert, I.: J. Phys. (Paris) Colloq. Suppl. 12, **47**, C8–569 (1986)
31. Schnopper, H.W.: Phys. Rev. **131**, 2558 (1963);
Bonnelle, C., Wuilleumier, F.: C.R. Acad. Sci. **256**, 510 (1963);
Deslattes, R.D., LaVilla, R.E., Cowan, P.E., Henins, A.: Phys. Rev. A **27**, 923 (1983)
32. Cooper, J.W.: Phys. Rev. A **38**, 3417 (1988)
33. Ginter, M.L., Tilford, S.J.: J. Mol. Spectrosc. **34**, 206 (1970)
34. Moeller, T., Jordan, B., Gürtler, P., Zimmerer, G., Haaks, D., Le Calvé, J., Castex, M.C.: Chem. Phys. **76**, 295 (1983)
35. Cederbaum, L.S., Tarantelli, F., Sgamelotti, A., Schirmer, J.: J. Chem. Phys. **86**, 2168 (1987)